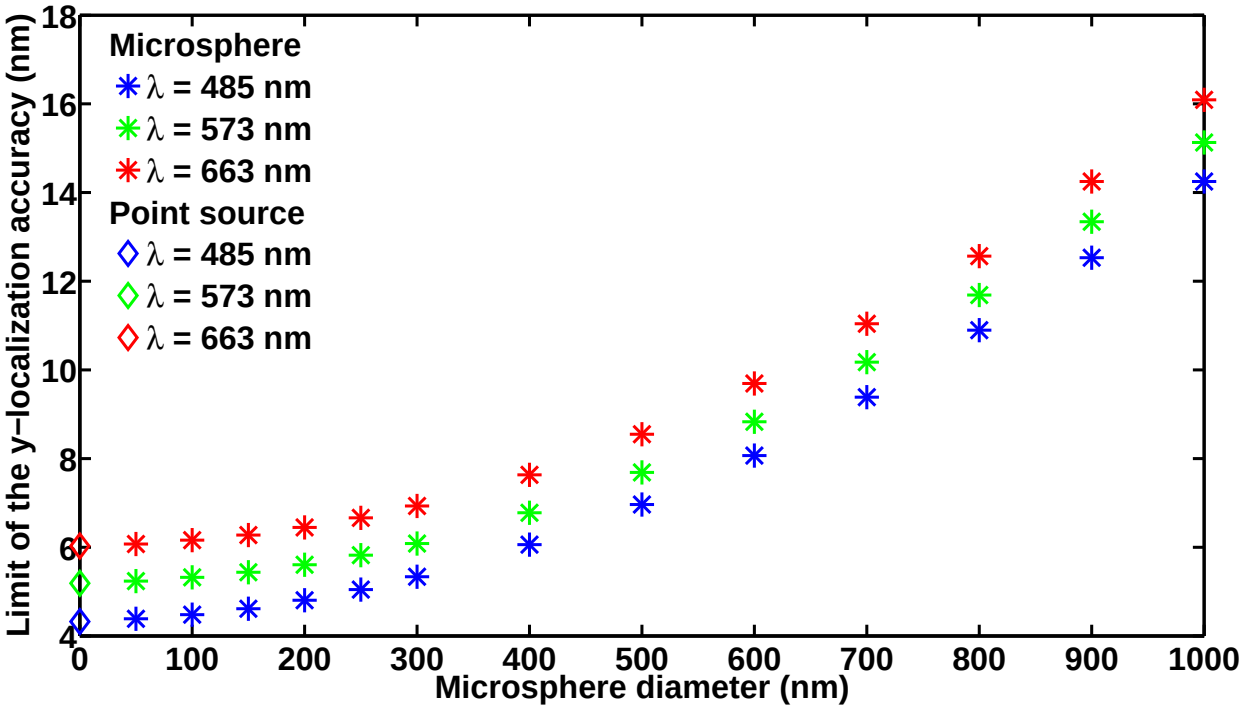

S1 Fig. Limit of the y-localization accuracy as a function of microsphere diameter. Limits are shown for microspheres that emit photons of wavelengths 485 nm, 573 nm, and 663 nm, imaged using the 63× imaging configuration specified in the section *Simulation parameters*. Values of all parameters not explicitly provided here, including the region of interest, the location of the microsphere, and the camera readout noise standard deviation used to compute the limits, are as given in the section *Simulation parameters*. For comparison, the limit of the y-localization accuracy for the point source that is located at the same position, and emits photons of the same wavelength, as the microsphere, is shown at the diameter of 0 nm.

S1 Table. Averages of the x_0 and y_0 estimates from the localization of Fluoresbrite microspheres with a fixed width Airy pattern.

Microsphere diameter (nm)	Data Set #	Mean of x_0 estimates (nm)	Mean of y_0 estimates (nm)
50	1	1537.69	1533.70
	2	1562.22	1528.57
	3	1552.94	1466.64
	4	1599.32	1559.95
	5	1577.28	1569.80
100	1	1536.66	1537.62
	2	1510.53	1578.71
	3	1565.68	1550.60
	4	1523.35	1608.88
	5	1612.13	1498.62
200 (190)	1	1576.14	1523.46
	2	1569.37	1577.35
	3	1611.50	1536.93
	4	1591.09	1521.24
	5	1544.32	1577.02
300 (320)	1	1639.24	1530.42
	2	1456.59	1522.76
	3	1459.01	1506.02
	4	1532.00	1585.90
	5	1521.72	1560.48
500	1	1627.25	1612.68
	2	1529.42	1632.22
	3	1464.13	1601.27
	4	1533.33	1480.54
	5	1536.31	1476.85
1000 (908)	1	1513.19	1640.41
	2	1607.35	1606.11
	3	1677.91	1556.38
	4	1562.32	1536.24
	5	1568.61	1499.40

The average values shown pertain to the data sets presented in Table 4.

S1 Text

Larger microspheres are more difficult to localize

Fig. 2 shows that for a given color, the limit of the localization accuracy deteriorates (i.e., increases in value) with increasing microsphere diameter, assuming the average number of microsphere photons detected over the detector plane is the same regardless of the microsphere's size. This is expected because a larger diameter yields a broader image profile (see, e.g., Fig. 1), and a broader image profile makes it more difficult to pinpoint the position of the underlying object. The latter assertion is supported, for example, by the simple expressions given in [13, 16] for the limit of the accuracy for localizing an in-focus point source imaged under ideal conditions. These expressions clearly show that the best possible accuracy for localizing the point source worsens when the width of its image profile, modeled as an Airy pattern or a 2-dimensional Gaussian function, is increased. Intuitively, one can also see that a higher localization uncertainty should be expected with a broader image profile because the positional coordinates of the underlying object lie within, and therefore must be extracted from, a flatter peak of some 2-dimensional surface. Note, however, that while larger microspheres may be more difficult to localize than smaller microspheres given the same average photon count, in practice more photons can typically be detected from larger microspheres under the same experimental conditions to significantly improve the localization accuracy (see, e.g., the experimental results reported in Tables 4 and 5). The fact that the estimation accuracy can be improved by detecting more photons from the object of interest is a well-known result [15, 16].

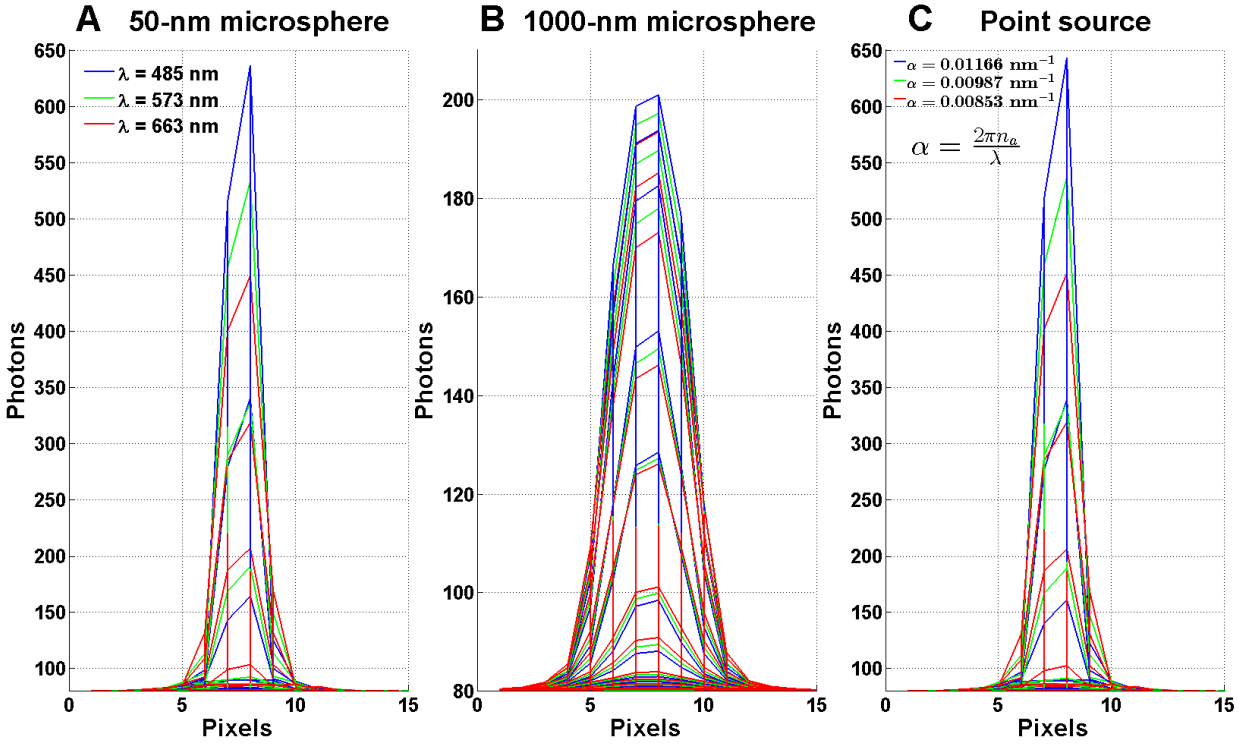

S2 Fig. Comparison of images at different wavelengths. Mesh representations of (A) images of 50-nm microspheres, (B) images of 1-μm microspheres, and (C) Airy patterns at wavelengths of 485 nm, 573 nm, and 663 nm are shown overlaid in different colors. The microspheres and point sources are assumed to be imaged using the 63× imaging configuration specified in the section *Simulation parameters*, and the images shown provide the view along the x-axis. Values of all relevant parameters not explicitly provided here are as given in the section *Simulation parameters*.

S2 Table. Averages of the x_0 and y_0 estimates from the localization of Fluoresbrite microspheres with a floated width Airy pattern.

Microsphere diameter (nm)	Data Set #	Mean of x_0 estimates (nm)	Mean of y_0 estimates (nm)
50	1	1537.54	1533.93
	2	1562.21	1528.90
	3	1553.07	1466.18
	4	1599.58	1560.45
	5	1577.10	1569.31
100	1	1536.71	1537.71
	2	1510.39	1579.69
	3	1565.79	1550.67
	4	1523.44	1608.54
	5	1613.26	1497.54
200 (190)	1	1576.65	1523.36
	2	1569.94	1578.11
	3	1611.98	1537.23
	4	1593.33	1522.03
	5	1544.86	1578.83
300 (320)	1	1639.36	1531.62
	2	1456.66	1526.02
	3	1460.50	1509.30
	4	1533.11	1588.27
	5	1519.92	1565.25
500	1	1624.69	1612.24
	2	1528.73	1636.19
	3	1466.82	1599.17
	4	1536.91	1483.24
	5	1540.11	1491.10
1000 (908)	1	1516.16	1635.19
	2	1585.78	1572.54
	3	1654.43	1588.06
	4	1585.59	1570.04
	5	1586.63	1491.37

The average values shown pertain to the data sets presented in Table 5.

S2 Text

Longer emission wavelength yields poorer localization accuracy

For a given microsphere diameter, it can be seen in Fig. 2 that the longer the wavelength of the photons detected from the microsphere, the worse the limit of the localization accuracy. This can be attributed to the fact that increasing the wavelength broadens the image profile of the microsphere, thereby making the microsphere's position more difficult to determine (see S1 Text). The broadening of the image profile with increasing wavelength is illustrated in S2 Fig. A and S2 Fig. B for a 50-nm and a 1-μm microsphere, respectively. In each case, the broadening of the profile can perhaps be better appreciated by observing the decrease in the height of the image profile as the wavelength is increased.

Fig. 2 further demonstrates that for smaller microspheres, the limit of the localization accuracy depends on the wavelength in a more substantial way. The x_0 coordinate of a 200-nm microsphere, for example, can be estimated with a best possible accuracy of 4.64 nm when the microsphere emits photons of wavelength 485 nm, but with a best possible accuracy of only 6.45 nm when photons of the longer wavelength 663 nm are emitted. The latter accuracy is worse than the former by 39%. Conversely, for larger microspheres, the limit of accuracy depends on the wavelength to a lesser extent. For the largest diameter of 1 μm considered here, for example, the best possible accuracy of 16.09 nm at the 663-nm wavelength is worse than the best possible accuracy of 14.24 nm at the 485-nm wavelength by a considerably smaller 13%.

The greater effect of wavelength at the smaller sizes is a result of the more significant change in the width (readily seen as a more significant change in the height) of the image profile when the wavelength is changed. This is evident when comparing the relatively big differences in the heights of the three image profiles for the 50-nm microsphere in S2 Fig. A with the relatively small differences in the heights of the three profiles for the 1-μm microsphere in S2 Fig. B. The more pronounced effect for a small microsphere is expected based on its image's similarity to an Airy pattern, the width of which is determined by the wavelength via its width parameter. S2 Fig. C, for example, shows the value of an Airy pattern's width parameter to decrease with increasing wavelength, resulting in a broadening of the pattern. Note how closely the 50-nm microsphere's profiles in S2 Fig. A resemble the Airy patterns in S2 Fig. C.

The relatively small effect of wavelength on the accuracy for localizing larger microspheres is due to the width of the image of a large microsphere being more a function of the microsphere's physical dimensions than a function of the wavelength of the microsphere's photons. This can be seen in S2 Fig. B, which again illustrates that changing the wavelength does relatively little in terms of altering the width of the image of a 1-μm microsphere. A more intuitive explanation is simply that the color of a relatively large object has little effect on the shape of the object's image, and hence little effect on how well the position of the object can be estimated.

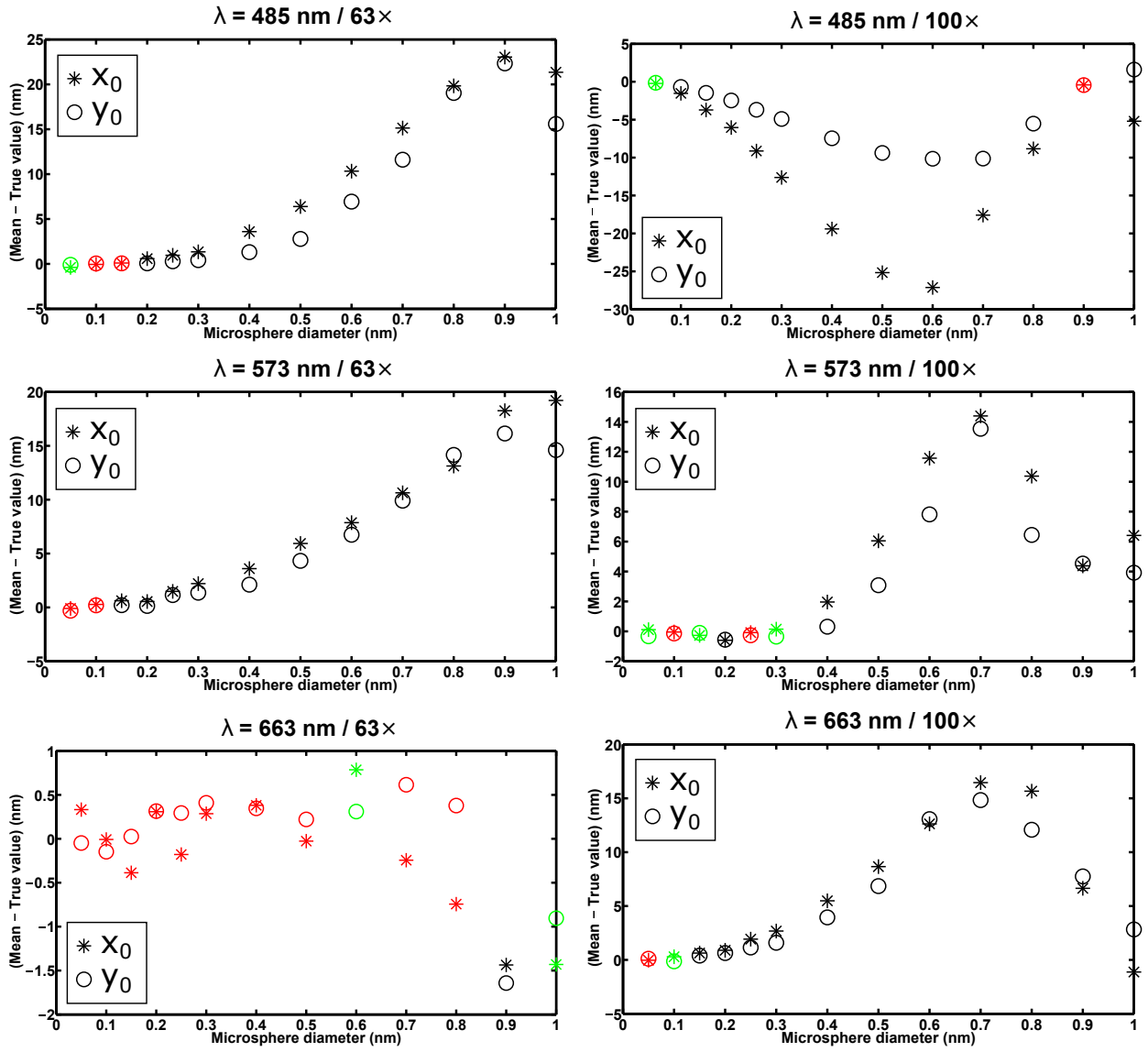

S3 Fig. Analysis of the mean of estimates from the maximum likelihood localization of microspheres with a fixed width Airy pattern - second set of data sets statistically identical to the data sets of Figs. 3 through 6. Each plot shows the results for 13 data sets, each consisting of 1000 repeat images of a microsphere of a different size, simulated with parameters corresponding to one of six combinations of wavelength and imaging configuration (see the section *Simulation parameters*). Each image in a data set was fitted with an Airy pattern whose positional coordinates x_0 and y_0 were estimated, but whose width parameter α was fixed to the value determined by the numerical aperture and wavelength used to generate the data set. For each data set, the differences between the mean of the x_0 estimates and the true value x_0, and between the mean of the y_0 estimates and the true value y_0, are plotted in green and red if both of their magnitudes are within 3 and 2 times, respectively, their respective standard errors of the mean for an ideal estimator.

S3 Text

Complete view of simulated data generation and analysis

Simulated microsphere and point source data sets were generated using the procedure of the section *Image simulation*, with settings as specified for the six combinations of wavelength and imaging configuration detailed in the section *Simulation parameters*. Each image in a given data set was subjected to maximum likelihood localization that fits an Airy pattern to the image, the details of which are given in the section *Maximum likelihood localization*. After discarding any pairs of x_0 and y_0 estimates that place the microsphere or point source outside the ROI used for the localization, the mean of the x_0 estimates and the mean of the y_0 estimates were calculated, and respectively compared to the true values x_0 and y_0. Likewise, the x-localization accuracy and the y-localization accuracy for the data set were calculated as the standard deviations of the x_0 estimates and the y_0 estimates, and respectively compared to the limits of the x- and y-localization accuracy, computed as described in the sections *Localization accuracy and its limit* and *The Airy pattern* for microsphere data and point source data, respectively.

Two types of localization were carried out on each data set. In one case, the width parameter of the Airy pattern was not estimated during the maximum likelihood localization, and was instead fixed to its theoretical value of $\frac{2\pi n_a}{\lambda}$, with n_a and λ as determined by the assumed imaging settings. In the other case, the width parameter was estimated along with the positional coordinates of the microsphere or point source, such that the maximum likelihood estimator was able to narrow or broaden the Airy pattern.

In both cases, the initial guesses for x_0 and y_0 were randomly generated, for each image in the data set, to be within $\pm 15\%$ of x_0 and y_0, respectively. This translates to initial guesses that are within approximately one pixel of the true value in both the x and y directions. In the case where the Airy width parameter was estimated, the initial guess for the width parameter was likewise randomly generated, for each image in the data set, to be within $\pm 15\%$ of the true (i.e., theoretical) value in the analysis of point source data sets. In the analysis of microsphere data sets, however, the initial guess for the Airy width parameter was the same for every image in the data set, and was determined by visually matching an Airy pattern to the model image of the microsphere.

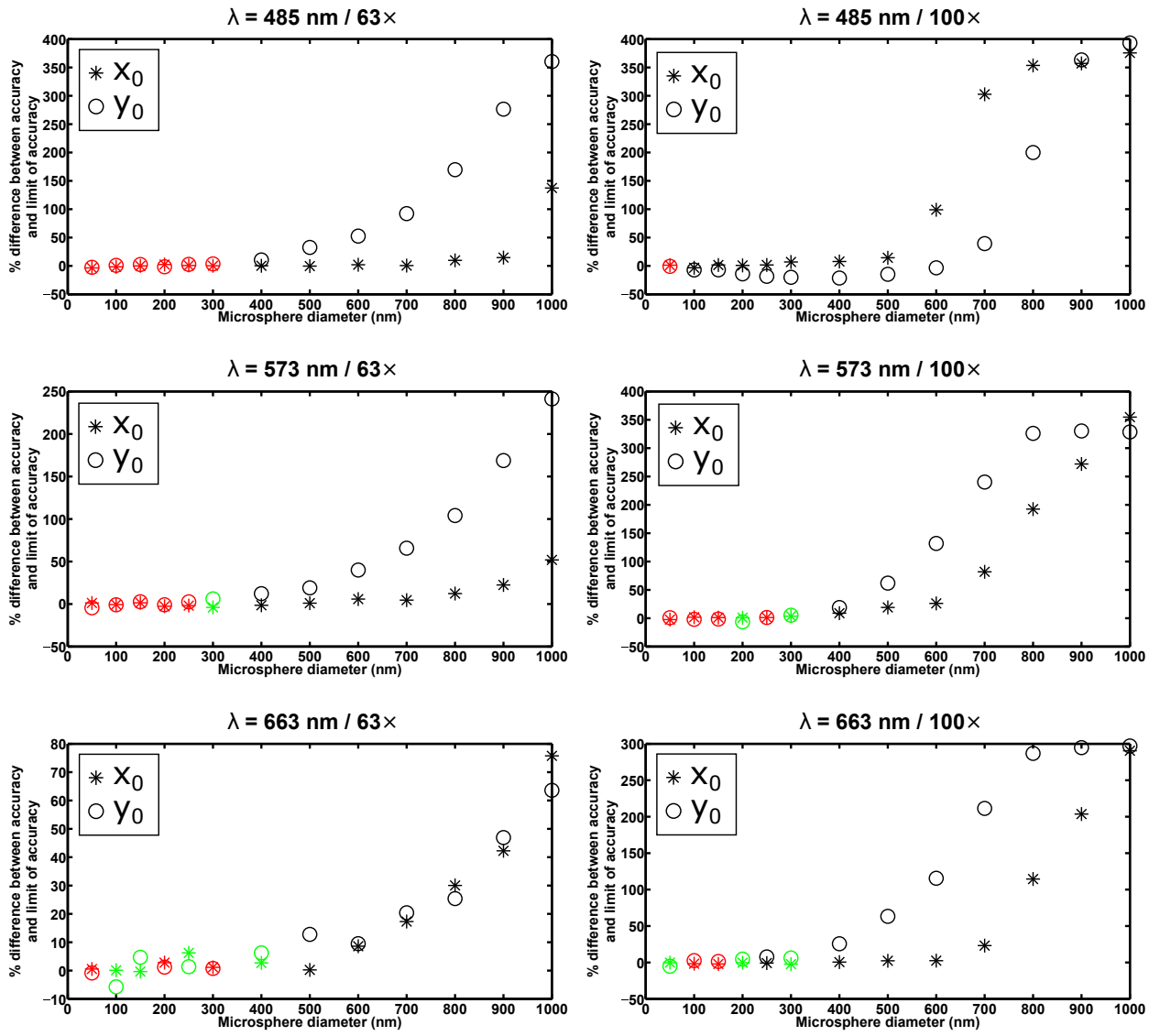

S4 Fig. Analysis of the accuracy (i.e., the standard deviation) of estimates from the maximum likelihood localization of microspheres with a fixed width Airy pattern - second set of data sets statistically identical to the data sets of Figs. 3 through 6. The results shown are for the same x_0 and y_0 estimates whose averages are analyzed in S3 Fig. For each data set, the percentage differences between the x-localization accuracy and the limit of the x-localization accuracy, and between the y-localization accuracy and the limit of the y-localization accuracy, are plotted in green and red if the corresponding absolute differences between the square of the localization accuracy (i.e., the variance of the estimates) and the square of the limit of accuracy are both within 3 and 2 times, respectively, their respective standard errors of the variance for an ideal estimator. The percentages are specified with respect to the limit of accuracy.

S4 Text

Complete view of experimental data generation and analysis

Each experimental data set consisted of repeat images of an in-focus microsphere, acquired as described in the section *Experimental image acquisition*. Prior to analysis, each image's pixel values were converted to units of photons by subtracting the camera offset and then multiplying by the gain conversion factor.

As in the case of the simulated data, each image in a given experimental data set was subjected to the maximum likelihood fitting of an Airy pattern as described in the section *Maximum likelihood localization*, and the x- and y-localization accuracies computed from the x_0 and y_0 estimates (after elimination of any pairs of x_0 and y_0 estimates that place the microsphere outside the ROI used for the localization) were respectively compared to the limits of the x- and y-localization accuracy (see the section *Localization accuracy and its limit*). More precisely, the localization was performed on a 15×15-pixel ROI on which the image of the microsphere was approximately centered, and the limits of accuracy, too, were calculated based on the ROI. Note, however, that the localization accuracies and their corresponding limits were computed based on estimates that were first corrected for drift of the microsphere sample with respect to the CCD camera. Drift-corrected x_0 estimates were obtained by fitting a cubic polynomial to the x_0 estimates to generate a drift curve, and then subtracting that curve from the x_0 estimates. Drift-corrected y_0 estimates were obtained independently in analogous fashion.

Also as in the case of the simulated data, each experimental data set was localized in two different ways - with and without the estimation of the Airy pattern's width parameter along with the positional coordinates of the microsphere. In the latter case, the width parameter of the Airy pattern was fixed to 0.00911 nm^{-1}, the average value of the width parameters estimated in the former case from the five 50-nm microsphere data sets. This average value makes a reasonable choice because of the high degree of similarity between the image of a 50-nm microsphere and the image of its corresponding point source.

For every image in a data set, the initial guesses for x_0 and y_0 were set to be the coordinates of the center of the ROI. In the case where the Airy width parameter was estimated, with the exception of the 1-μm microsphere data sets, the initial guess for the width parameter was set to the theoretical value $\frac{2\pi n_a}{\lambda}$, with $n_a = 1.4$ and $\lambda = 485$ nm, based on the objective lens and emission filter used for the image acquisition (see the section *Experimental image acquisition*). For the 1-μm microsphere data sets, the initial guess was set to the much broader width of 0.003 nm^{-1}, as we found the estimator to have trouble broadening the Airy pattern to match the large width of the 1-μm microsphere when the theoretical value was used as the initial guess.

Unlike for the simulated data sets where values of parameters that are not estimated, but are required for the maximum likelihood localization, are known, for the experimental data sets the values of these parameters need to be separately determined. Values for the image pixel size, the objective magnification M, the refractive index n of the lens immersion medium, and

the mean η_0 and standard deviation σ_0 of the CCD camera's readout noise all depend solely on the acquisition setup and environment, and are given in the section *Experimental image acquisition*. Values for the mean photon count N_{photon} detected from a microsphere, and the mean photon count β_0 detected per pixel from the background component, however, depend on the particular microsphere sample in addition to the acquisition setup and environment, and were determined for each microsphere data set individually as follows.

For each experimental data set, we first verified that a constant signal level and a constant background level could be reasonably assumed over the course of time during which the data set was acquired. To do so, an ROI (not the relatively small 15×15-pixel ROI subsequently used for the maximum likelihood localization) was selected around the microsphere. This ROI was chosen to be as large as possible (without coming too close to a neighboring microsphere) in order to get a good approximation of the background level based on the values of the peripheral pixels of the ROI. Specifically, for each image in the data set, the background level was approximated as the average of the values of the pixels on the outermost rows and columns of the ROI. The stability of the rate at which background photons were detected during the data acquisition was then visually verified as a relatively even spread of points about their mean in a scatter plot of the background levels determined for the set of images. By the assumption of a spatially uniform background (justified by the relatively flat periphery of the ROI), for each image in the data set an approximation of the number of microsphere photons detected within the ROI was obtained by multiplying the background level for the image by the number of pixels comprising the ROI, and subtracting the result from the sum of the values of all pixels comprising the ROI. The stability of the rate at which microsphere photons were detected during the data acquisition was then visually verified as a relatively even spread of points about their mean in a scatter plot of the microsphere photon counts determined for the set of images.

Given the assumption of a constant signal level and a constant background level throughout the acquisition of a data set, the mean microsphere photon count N_{photon} and the mean per-pixel background photon count β_0 are the same for each image in the data set. To obtain estimates of these two parameters, we added all the images in the data set to produce a sum image on which the estimation was carried out. The summing of images is desirable because it increases the amount of data on which estimation is performed, thereby improving the accuracy with which a parameter can be estimated. Specifically, using our microsphere image model and MATLAB's *lsqnonlin* function, a nonlinear least squares optimization was carried out on the same ROI that was used for the verification of signal and background stability from the individual images. In the microsphere image model, the radius r was set to half the average diameter specified by the manufacturer for the particular microsphere sample, or to half the nominal diameter if the average diameter for the sample was different by no more than 2%. The quantities estimated consisted of the x_0 and y_0 coordinates of the microsphere, the term $\frac{2\pi n_a}{\lambda}$ of Eq. (5), and the parameters N_{photon} and β_0. Since the values obtained for N_{photon} and β_0 pertained to the sum image, they were each divided by the number of images in the data set, and the results were used as fixed values for N_{photon} and β_0 in the maximum likelihood localization carried out on each individual image of the data set.

For the calculation of the limits of the localization accuracy to which the obtained localization accuracies were compared, the positional coordinates x_0 and y_0 were given by the mean of the x_0 estimates and the mean of the y_0 estimates, respectively, since the true values are not known for the experimental data sets. The radius r was set to either half the sample's average diameter or half the nominal diameter as described above, and the term $\frac{2\pi n_a}{\lambda}$ was set to the value determined from the sum image by the nonlinear least squares estimation.

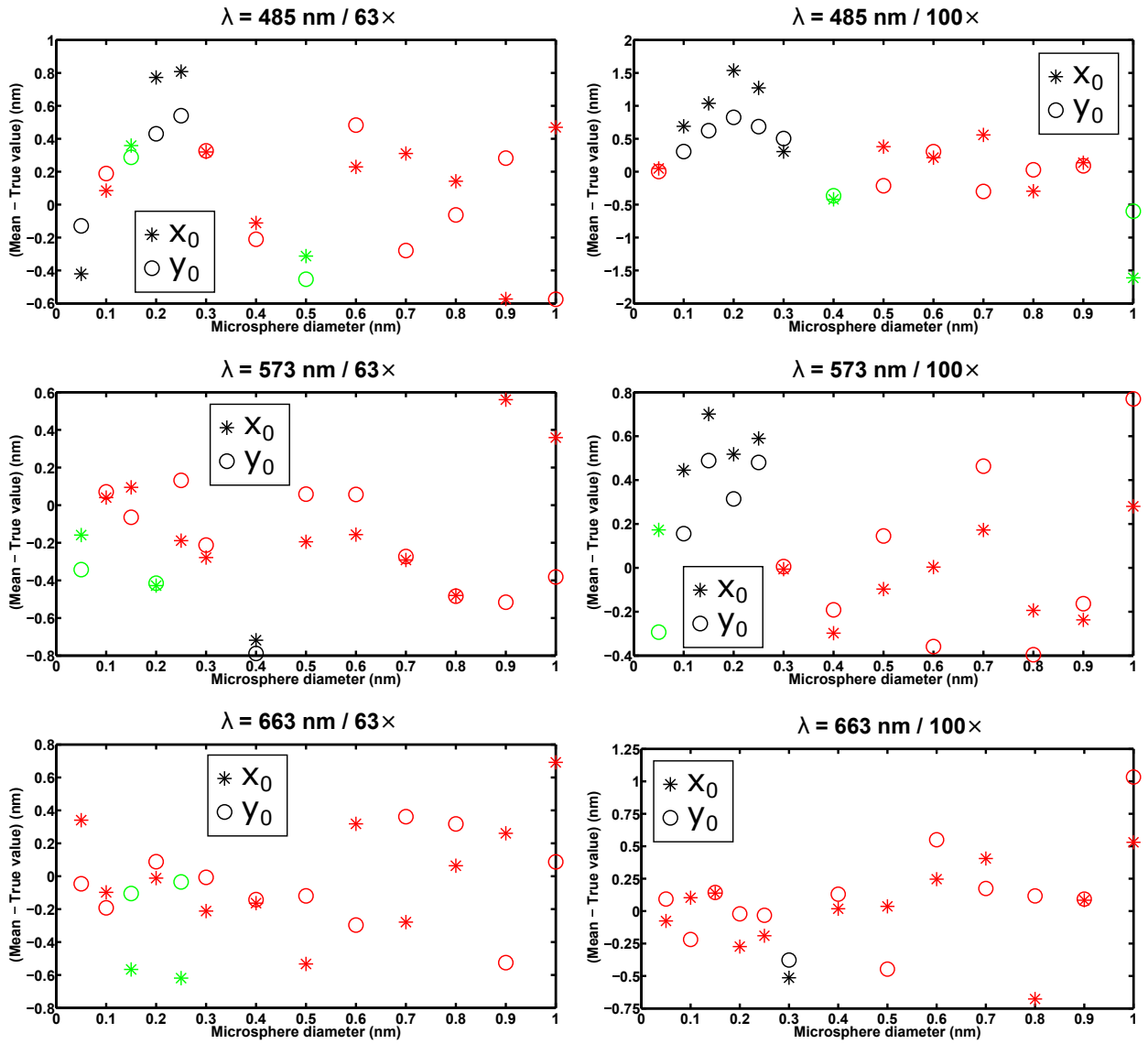

S5 Fig. Analysis of the mean of estimates from the maximum likelihood localization of microspheres with a floated width Airy pattern - second set of data sets statistically identical to the data sets of Figs. 3 through 6. The results shown are obtained from localization carried out on the same data sets as in S3 Fig, but with the width parameter of the fitted Airy pattern estimated along with its positional coordinates x_0 and y_0. For each data set, the differences between the mean of the x_0 estimates and the true value x_0, and between the mean of the y_0 estimates and the true value y_0, are plotted in green and red if both of their magnitudes are within 3 and 2 times, respectively, their respective standard errors of the mean for an ideal estimator.

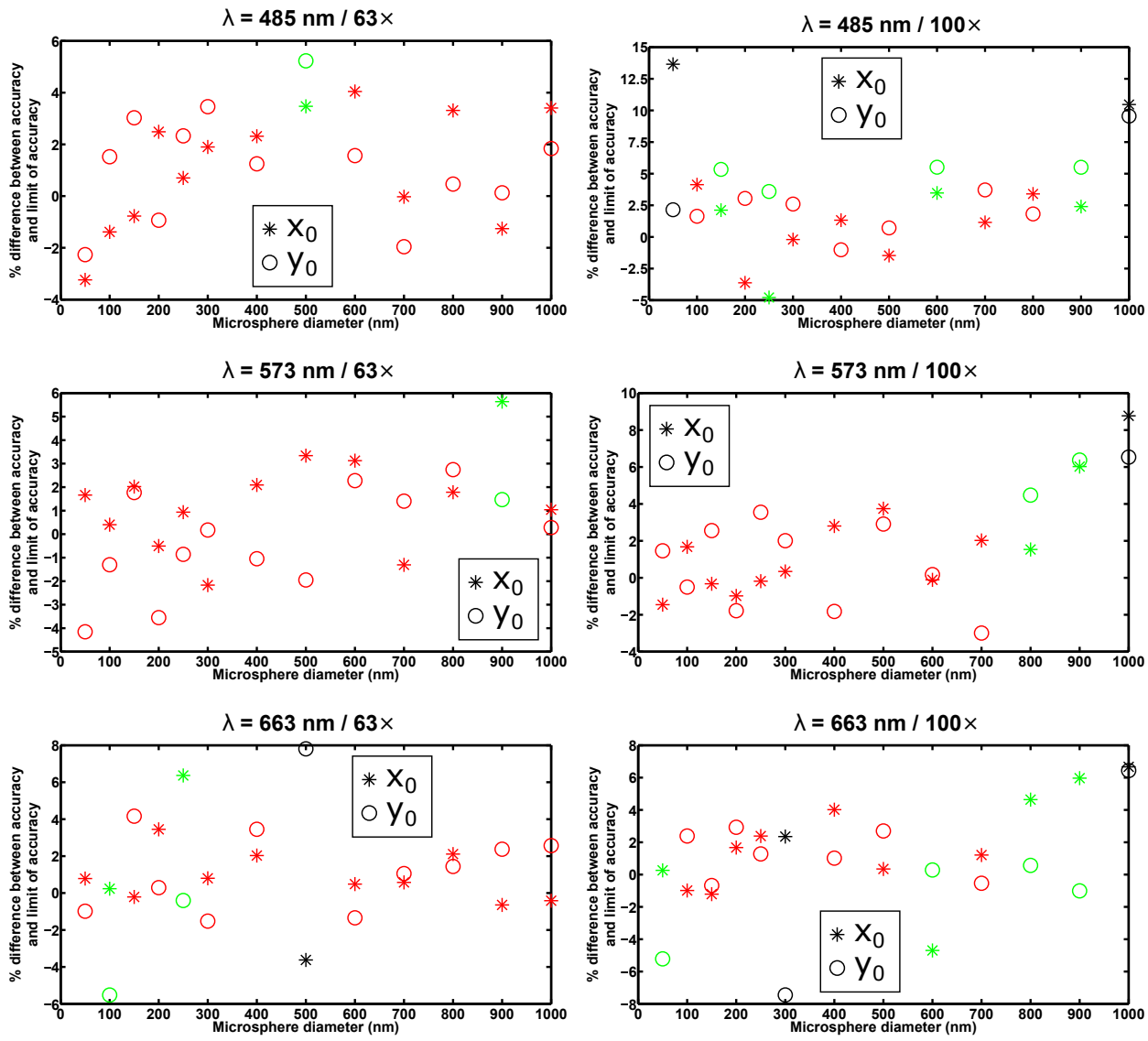

S6 Fig. Analysis of the accuracy (i.e., the standard deviation) of estimates from the maximum likelihood localization of microspheres with a floated width Airy pattern - second set of data sets statistically identical to the data sets of Figs. 3 through 6. The results shown are for the same x_0 and y_0 estimates whose averages are analyzed in S5 Fig. For each data set, the percentage differences between the x-localization accuracy and the limit of the x-localization accuracy, and between the y-localization accuracy and the limit of the y-localization accuracy, are plotted in green and red if the corresponding absolute differences between the square of the localization accuracy (i.e., the variance of the estimates) and the square of the limit of accuracy are both within 3 and 2 times, respectively, their respective standard errors of the variance for an ideal estimator. The percentages are specified with respect to the limit of accuracy.

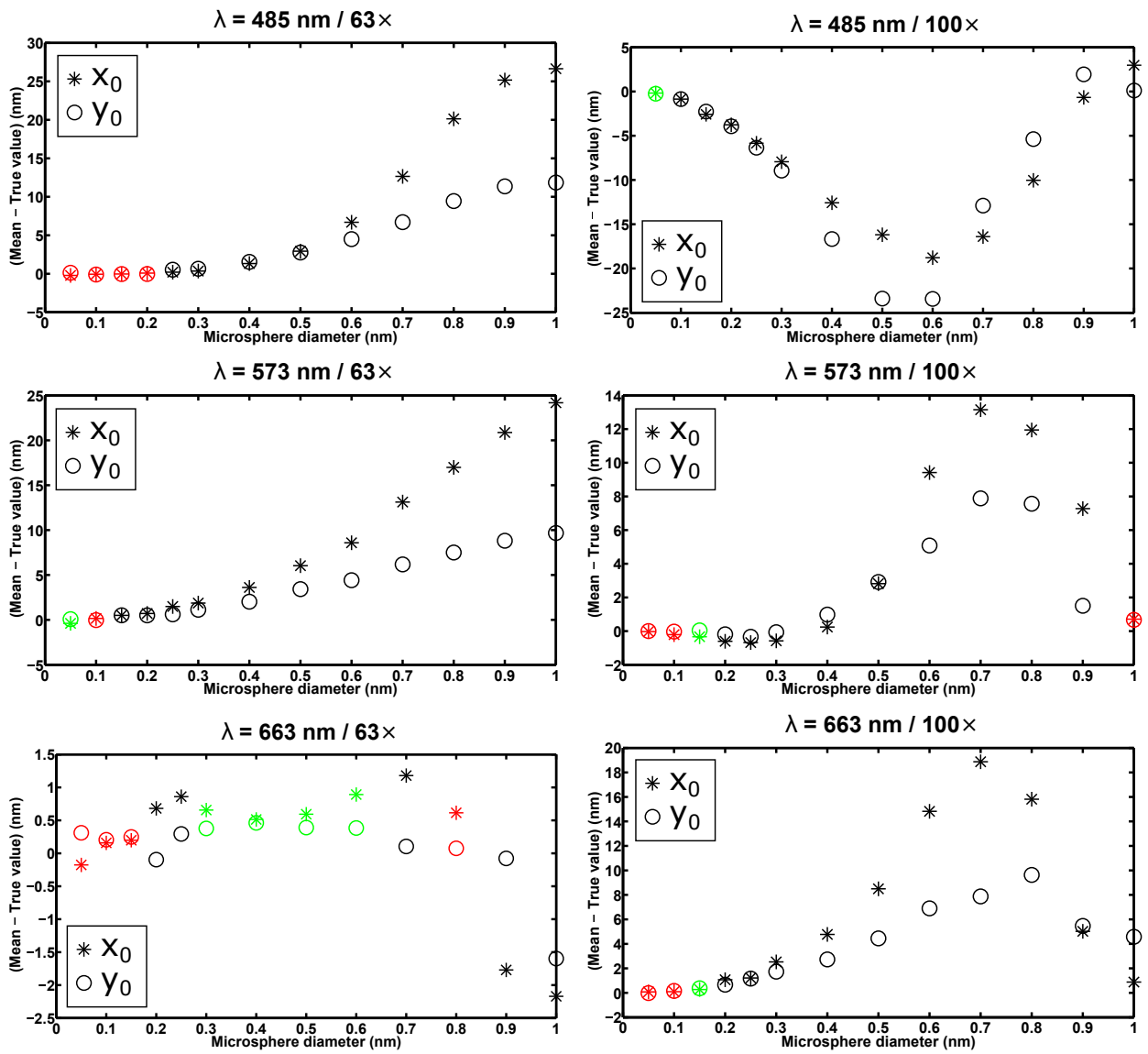

S7 Fig. Analysis of the mean of estimates from the maximum likelihood localization of microspheres with a fixed width Airy pattern - data sets with a different microsphere location. Each plot shows the results for 13 data sets, each consisting of 1000 repeat images of a microsphere of a different size, simulated with parameters corresponding to one of six combinations of wavelength and imaging configuration specified in the section *Simulation parameters*), except the microsphere location is set to 7.2 pixels in the x direction and 7.4 pixels in the y direction. Each image in a data set was fitted with an Airy pattern whose positional coordinates x_0 and y_0 were estimated, but whose width parameter α was fixed to the value determined by the numerical aperture and wavelength used to generate the data set. For each data set, the differences between the mean of the x_0 estimates and the true value x_0, and between the mean of the y_0 estimates and the true value y_0, are plotted in green and red if both of their magnitudes are within 3 and 2 times, respectively, their respective standard errors of the mean for an ideal estimator.

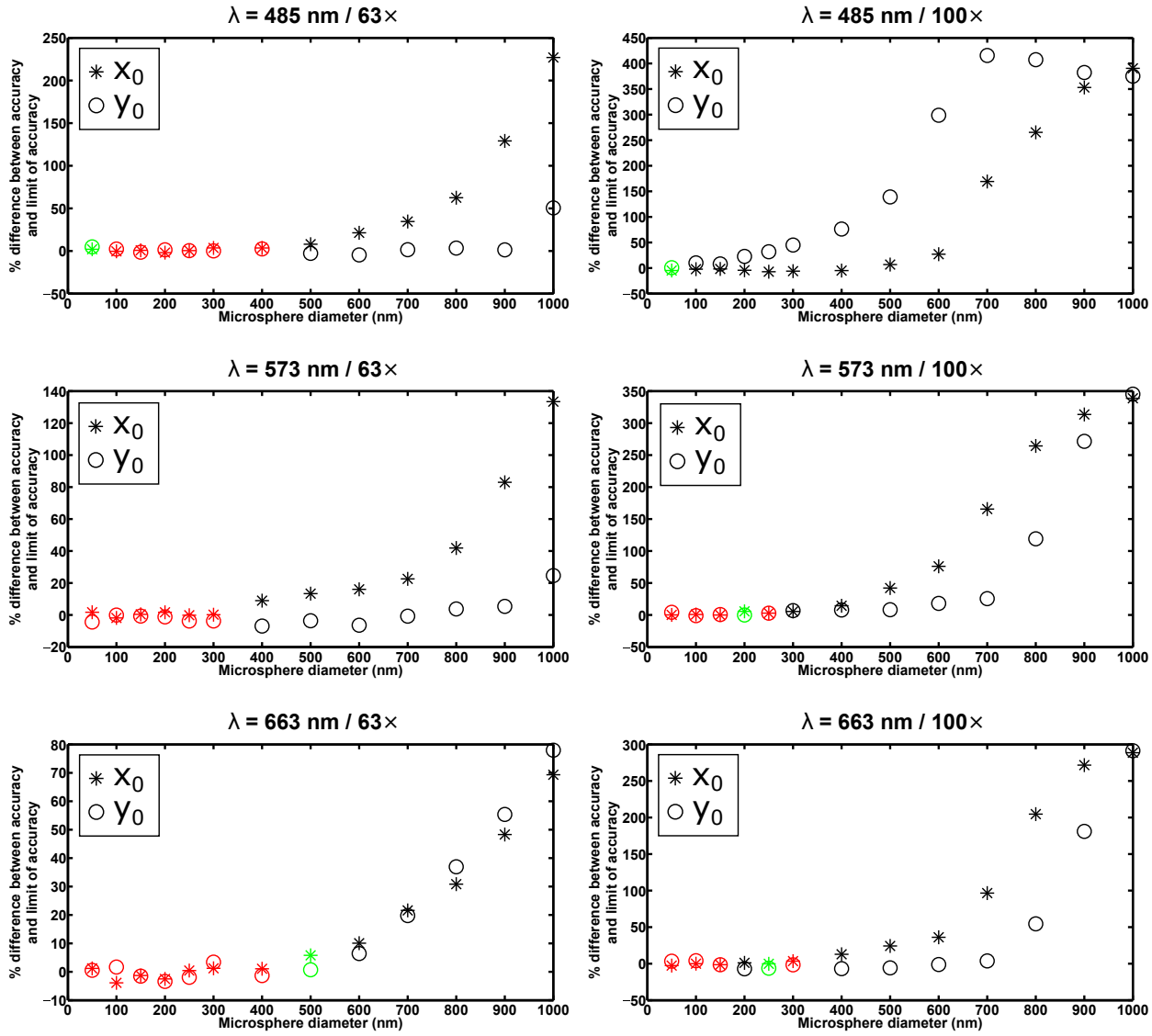

S8 Fig. Analysis of the accuracy (i.e., the standard deviation) of estimates from the maximum likelihood localization of microspheres with a fixed width Airy pattern - data sets with a different microsphere location. The results shown are for the same x_0 and y_0 estimates whose averages are analyzed in S7 Fig. For each data set, the percentage differences between the x-localization accuracy and the limit of the x-localization accuracy, and between the y-localization accuracy and the limit of the y-localization accuracy, are plotted in green and red if the corresponding absolute differences between the square of the localization accuracy (i.e., the variance of the estimates) and the square of the limit of accuracy are both within 3 and 2 times, respectively, their respective standard errors of the variance for an ideal estimator. The percentages are specified with respect to the limit of accuracy.

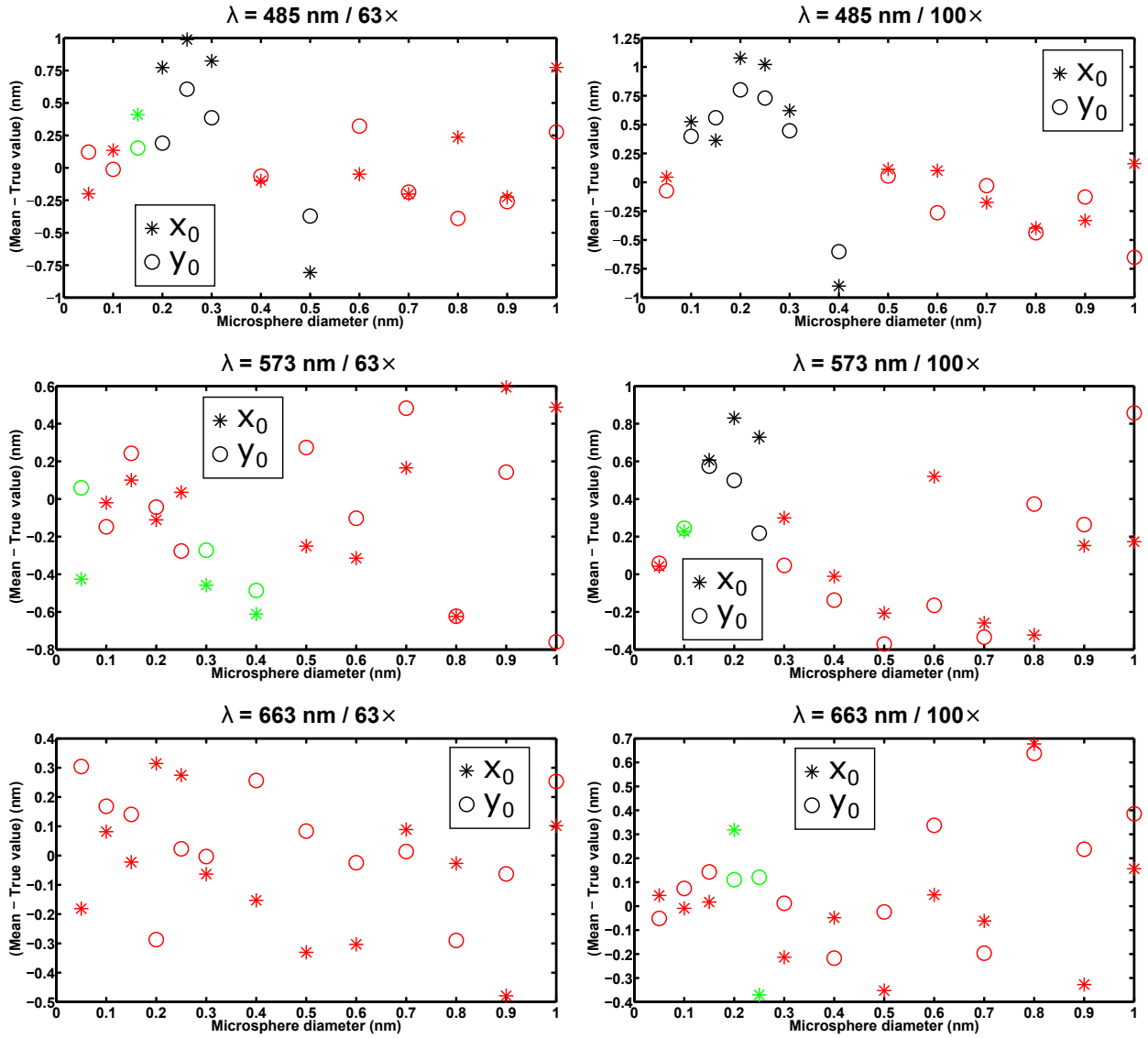

S9 Fig. Analysis of the mean of estimates from the maximum likelihood localization of microspheres with a floated width Airy pattern - data sets with a different microsphere location. The results shown are obtained from localization carried out on the same data sets as in S7 Fig, but with the width parameter of the fitted Airy pattern estimated along with its positional coordinates x_0 and y_0. For each data set, the differences between the mean of the x_0 estimates and the true value x_0, and between the mean of the y_0 estimates and the true value y_0, are plotted in green and red if both of their magnitudes are within 3 and 2 times, respectively, their respective standard errors of the mean for an ideal estimator.

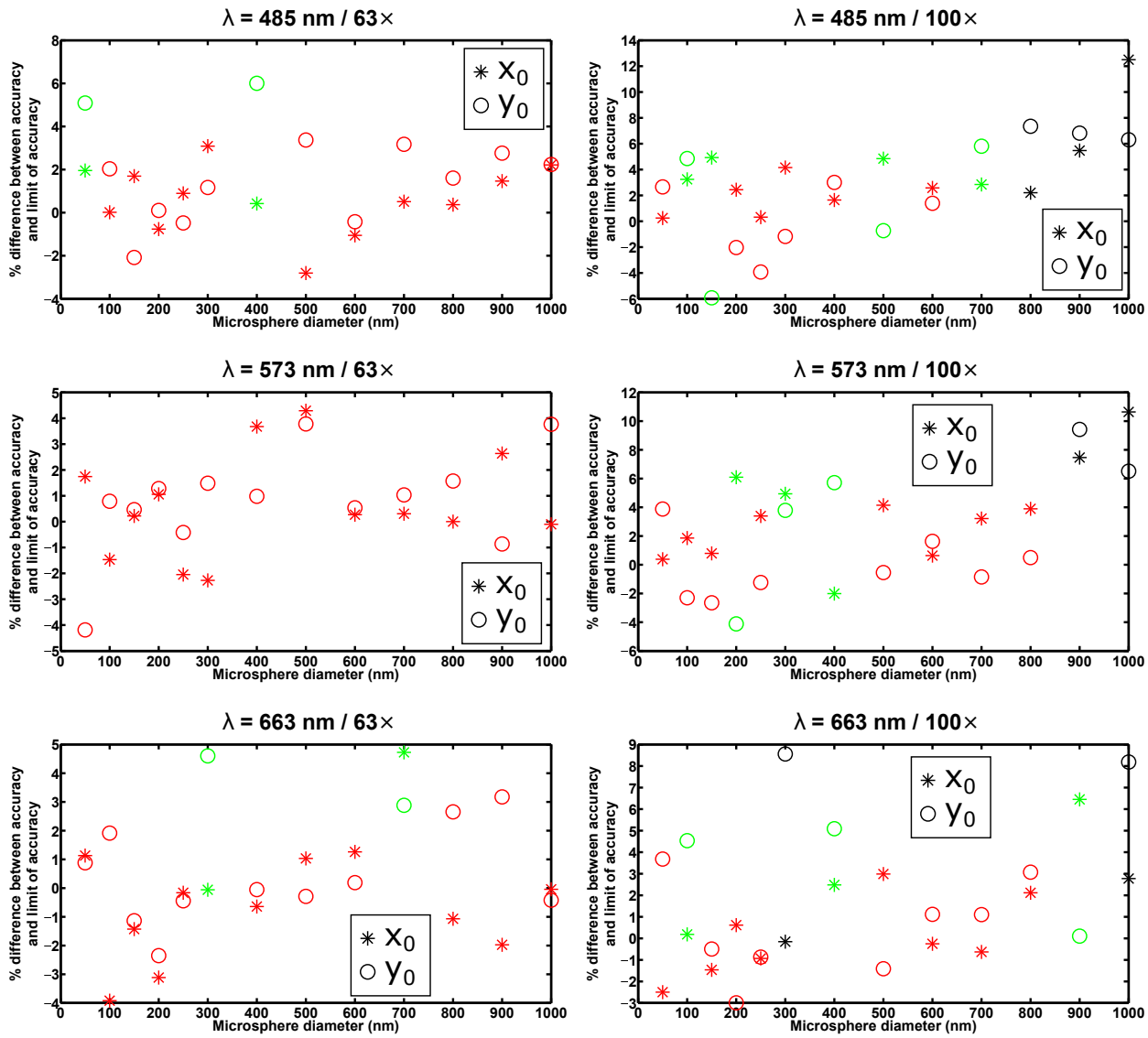

S10 Fig. Analysis of the accuracy (i.e., the standard deviation) of estimates from the maximum likelihood localization of microspheres with a floated width Airy pattern - data sets with a different microsphere location. The results shown are for the same x_0 and y_0 estimates whose averages are analyzed in S9 Fig. For each data set, the percentage differences between the x-localization accuracy and the limit of the x-localization accuracy, and between the y-localization accuracy and the limit of the y-localization accuracy, are plotted in green and red if the corresponding absolute differences between the square of the localization accuracy (i.e., the variance of the estimates) and the square of the limit of accuracy are both within 3 and 2 times, respectively, their respective standard errors of the variance for an ideal estimator. The percentages are specified with respect to the limit of accuracy.

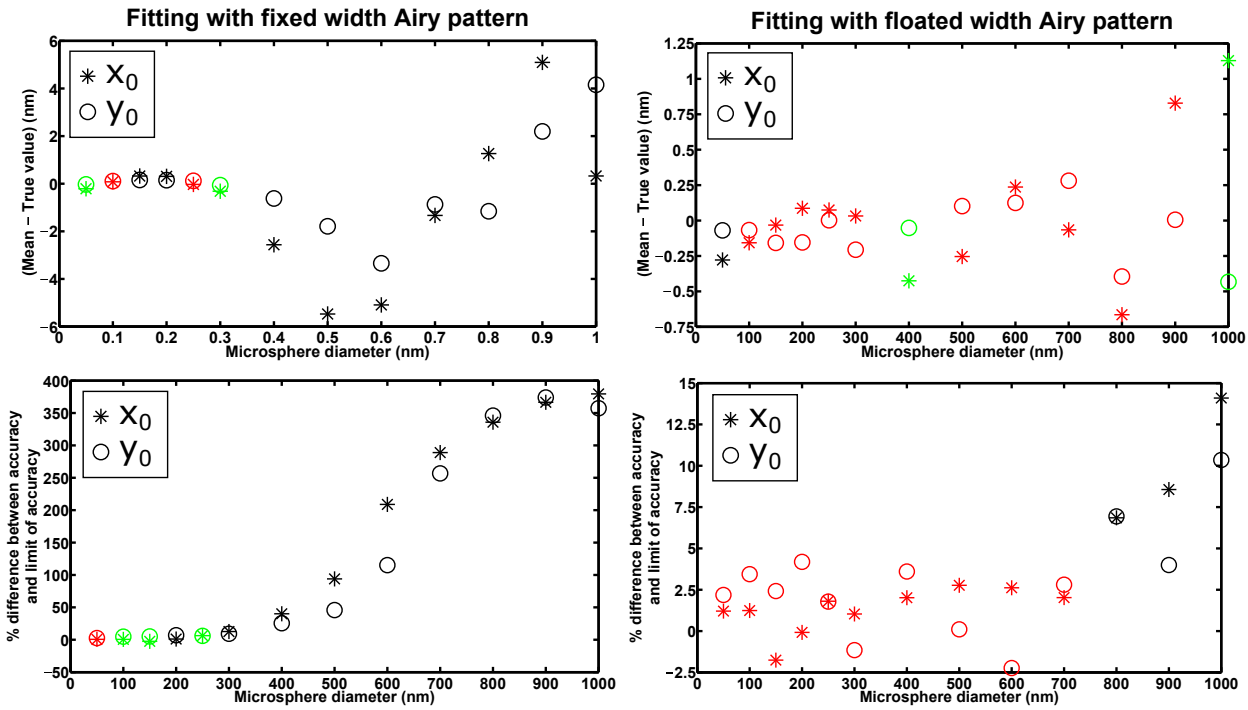

S11 Fig. Analysis of the mean and accuracy (i.e., standard deviation) of estimates from the maximum likelihood localization of microspheres with a fixed width (left-hand side plots) and a floated width (right-hand side plots) Airy pattern - second set of data sets statistically identical to the data sets of Fig. 7. Results are shown for 13 data sets, each consisting of 1000 repeat images of a microsphere of a different size, simulated with parameters specified in the section *Simulation parameters* for the $\lambda = 485$ nm / 100× combination, except the magnification has been changed to $M = 160$ to yield a smaller effective pixel size of 100 nm, the ROI and the per-pixel mean background photon count have accordingly been changed to a 21×21-pixel array and $\beta_0 = 30$, respectively, to retain the detection of similar numbers of photons from the microsphere and the background component, and the lateral location of the microsphere has been changed to 10.3 pixels in the x direction and 10.1 pixels in the y direction within the ROI. For each data set, the difference between the mean of estimates and the true value for each positional coordinate, and the percentage difference between the localization accuracy and the limit of the localization accuracy for each positional coordinate, are color-coded as in Figs. 3 through 6.

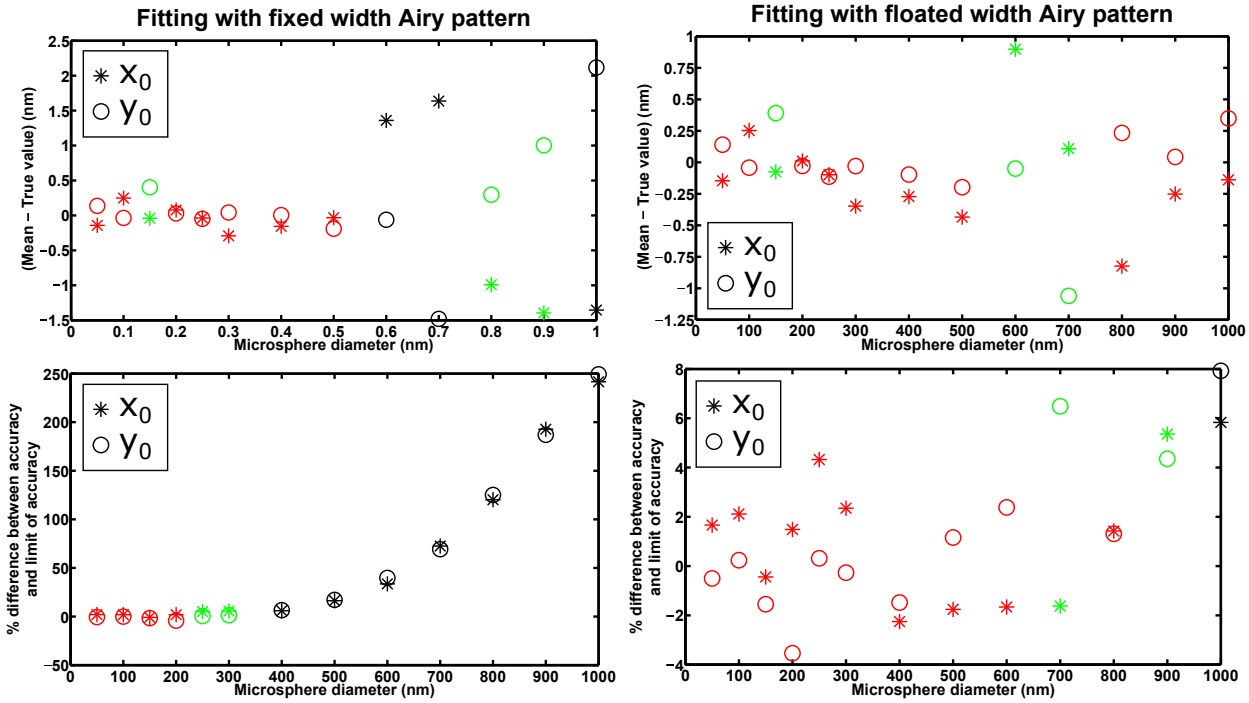

S12 Fig. Analysis of the mean and accuracy (i.e., standard deviation) of estimates from the maximum likelihood localization of microspheres with a fixed width (left-hand side plots) and a floated width (right-hand side plots) Airy pattern - finer pixelation for the $\lambda = 485$ nm / 63× combination. Results are shown for 13 data sets, each consisting of 1000 repeat images of a microsphere of a different size, simulated with parameters specified in the section *Simulation parameters* for the $\lambda = 485$ nm / 63× combination, except the magnification and pixel size have been changed to $M = 160$ and 16 μm × 16 μm to yield a smaller effective pixel size of 100 nm, the ROI and the per-pixel mean background photon count have accordingly been changed to a 21×21-pixel array and $\beta_0 = 30$, respectively, to retain the detection of similar numbers of photons from the microsphere and the background component, and the lateral location of the microsphere has been changed to 10.3 pixels in the x direction and 10.1 pixels in the y direction within the ROI. For each data set, the difference between the mean of estimates and the true value for each positional coordinate, and the percentage difference between the localization accuracy and the limit of the localization accuracy for each positional coordinate, are color-coded as in Figs. 3 through 6.

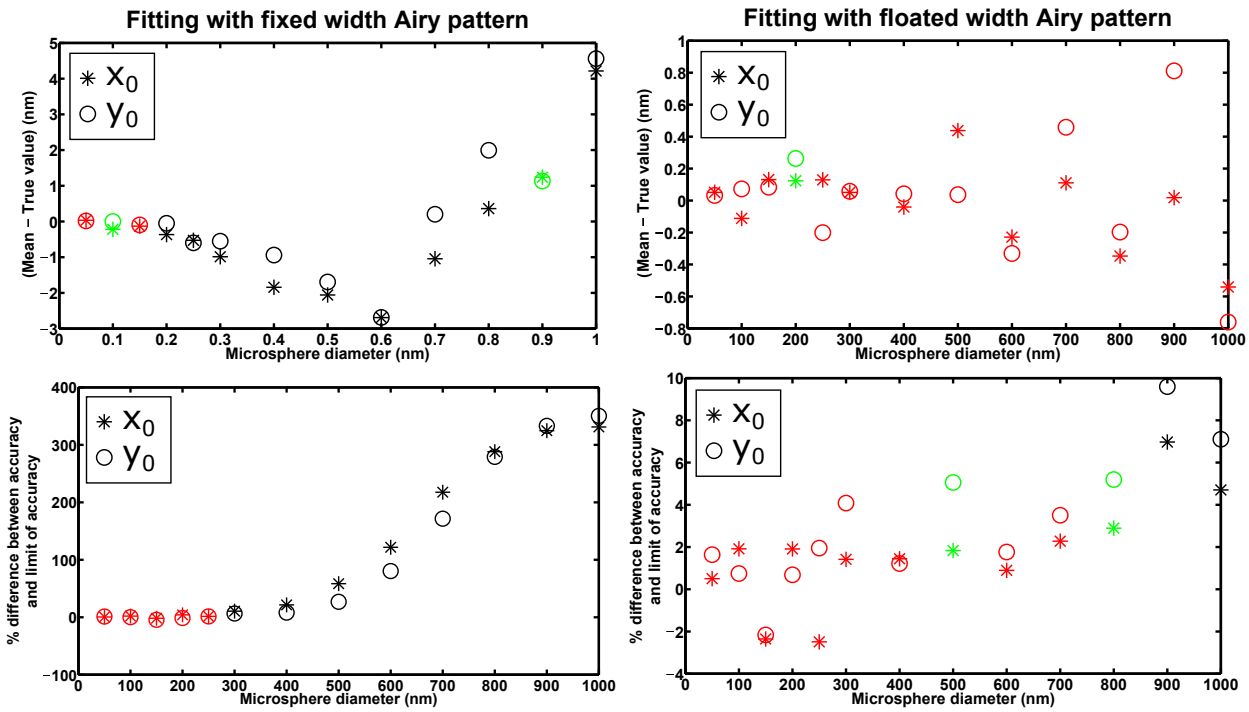

S13 Fig. Analysis of the mean and accuracy (i.e., standard deviation) of estimates from the maximum likelihood localization of microspheres with a fixed width (left-hand side plots) and a floated width (right-hand side plots) Airy pattern - finer pixelation for the $\lambda = 573$ nm / 100× combination. Results are shown for 13 data sets, each consisting of 1000 repeat images of a microsphere of a different size, simulated with parameters specified in the section *Simulation parameters* for the $\lambda = 573$ nm / 100× combination, except the magnification has been changed to $M = 160$ to yield a smaller effective pixel size of 100 nm, the ROI and the per-pixel mean background photon count have accordingly been changed to a 21×21-pixel array and $\beta_0 = 30$, respectively, to retain the detection of similar numbers of photons from the microsphere and the background component, and the lateral location of the microsphere has been changed to 10.3 pixels in the x direction and 10.1 pixels in the y direction within the ROI. For each data set, the difference between the mean of estimates and the true value for each positional coordinate, and the percentage difference between the localization accuracy and the limit of the localization accuracy for each positional coordinate, are color-coded as in Figs. 3 through 6.